ChemComm

Explore Short-Wavelength Birefringent Crystals via Triggering Cooperative Arrangement Between Different π-Conjugated Groups

Journal:	*ChemComm*
Manuscript ID	CC-COM-10-2024-005266.R1
Article Type:	Communication

ChemComm

COMMUNICATION

Explore Short-Wavelength Birefringent Crystals *via* Triggering Cooperative Arrangement Between Different π-Conjugated Groups

Received 00th January 20xx,
Accepted 00th January 20xx

DOI: 10.1039/x0xx00000x

Xiao Wang,[a] Tingwen Han,[a] Kenneth R. Poeppelmeier,[b] Xueling Hou,[c] Shilie Pan[c] and Fangfang Zhang*[a, c]

We herein reported our strategy to assemble planar π-conjugated $[B(OH)_3]$ and $[C_2O_4]^{2-}/[HC_2O_4]^{-}/[C_4O_4]^{2-}$ functional groups to explore short-wavelength birefringent crystals. Three compounds, $K_2C_2O_4{\cdot}B(OH)_3$, $Cs_4(HC_2O_4)_2(C_2O_4){\cdot}[B(OH)_3]_2$ and $K(C_4O_4)_{0.5}{\cdot}B(OH)_3$, which all exhibit a layered structure favorable for generating large optical anisotropy, were synthesized and characterized. The strategy of assembling π-conjugated $[B(OH)_3]$ and C–O functional modules shows the potential to explore promising UV birefringent materials.

Ordinary and extraordinary rays with different speeds will form when a beam of light is incident on birefringent crystals. Utilizing this phenomena, birefringent crystals can modulate the polarization of light, which play crucial roles in laser technology.[1,2] After decades of constant research, a variety of birefringent materials applied in the spectral regions from deep ultraviolet (DUV) to infrared (IR), such as MgF_2, α-BaB_2O_4, $CaCO_3$, YVO_4, and TiO_2, have been found.[3] However, these crystals still have drawbacks that limit their applications, and the investigation of novel birefringent materials, especially in the UV region, remain a significant challenge.[3,4]

Generally, the strategy for designing UV birefringent materials is to introduce functional units with a large polarization anisotropy.[5] For this reason, π-conjugated groups, such as CO_3^{2-}, BO_3^{3-}, NO_3^{-}, $B_3O_6^{3-}$, *etc*., are regarded as birefringence-active modules superior to non π-conjugated groups.[6,7] It is worth noting that π-conjugated C–O units, such as $[C_2O_4]^{2-}$, $[C_2O_6]^{2-}$, $[C_4O_4]^{2-}$ and $[C_6O_6]^{2-}$, were studied and are excellent birefringent modules for large polarization anisotropy.[8] The planar $[C_2O_4]^{2-}$ units exhibit a larger polarization anisotropy (21.87) than that of nonplanar $[C_2O_4]^{2-}$ (6.78), and the $[C_4O_4]^{2-}$ units consisting of a square ring of four C atoms exhibit a high degree of polarization anisotropy (51.52).[8] Considering the relationship between crystal structure and performance, the functional groups should arrange parallel in the lattice as possible, which can enhance the optical anisotropy of compounds. Regrettably, in some reported compounds with C–O units, such as $C(NH_2)_3(HC_4O_4)$,[9] $CsHC_2O_4$[10] and $Cs(HC_2O_4)(H_2C_2O_4){\cdot}2H_2O$,[11] the π-conjugated C–O units do not achieve a uniform parallel arrangement, which is still a common problem of designing UV birefringent materials. Thus it is important to propose an effective strategy to rationally regulate these functional groups.

$[B(OH)_3]$, the derivative of π-conjugated $[BO_3]$ unit, whose hydrogen bonding interactions in the coordinated linkers may aid in the optimal arrangements of anionic groups. For example, we noticed that in the following compounds, $Na_2C_4O_4(H_3BO_3)(H_2O){\cdot}H_3BO_3$ (0.26@1064 nm),[12] $(NH_4)_3[B(OH)_3]_2(COOH)_3$ (0.156@546 nm),[13] $Rb_3(COOH)_3(H_3BO_3)_2$ (0.09@1064 nm)[14] and $Cs_3(COOH)_3(H_3BO_3)_2$ (0.10@1064 nm),[14] their $[B(OH)_3]$ units remain in a planar arrangement with the C–O units, and they all exhibit large birefringence. However, the regulatory role of $[B(OH)_3]$ units on cooperative arrangement has not been adequately researched.

Herein, we tried to assemble π-conjugated C–O units by the use of $[B(OH)_3]$ units to design UV birefringent materials. Three new compounds, $K_2C_2O_4{\cdot}B(OH)_3$ (**Ⅰ**), $Cs_4(HC_2O_4)_2(C_2O_4){\cdot}[B(OH)_3]_2$ (**Ⅱ**) and $K(C_4O_4)_{0.5}{\cdot}B(OH)_3$ (**Ⅲ**) were successfully synthesized. The regulation of $[B(OH)_3]$ on crystal structure and optical performances are and discussed based on experimental characterizations and theoretical calculations.

[a] *College of Materials Science and engineering, Xinjiang University, Urumqi 830017, China*
[b] *Department of Chemistry, Northwestern University, 2145 Sheridan Road, Evanston, Illinois 60208-3113, United States*
[c] *Research Center for Crystal Materials, State Key Laboratory of Functional Materials and Devices for Special Environmental Conditions, Xinjiang Key Laboratory of Functional Crystal Materials, Xinjiang Technical Institute of Physics and Chemistry of CAS, 40-1 South Beijing Road, Urumqi 830011, China*
*To whom correspondence should be addressed, E-mail: ffzhang@ms.xjb.ac.cn
†Electronic supplementary information (ESI) available: CIF files; atomic coordinates and equivalent isotropic displacement parameters; selected bond lengths and angles; CCDC 2373841, 2373842 and 2373843 for $K_2C_2O_4{\cdot}B(OH)_3$, $K(C_4O_4)_{0.5}{\cdot}B(OH)_3$ and $Cs_4(HC_2O_4)_2(C_2O_4){\cdot}[B(OH)_3]_2$. For ESI and crystallographic data in CIF see DOI: 10.1039/x0xx00000x.

ChemComm

COMMUNICATION

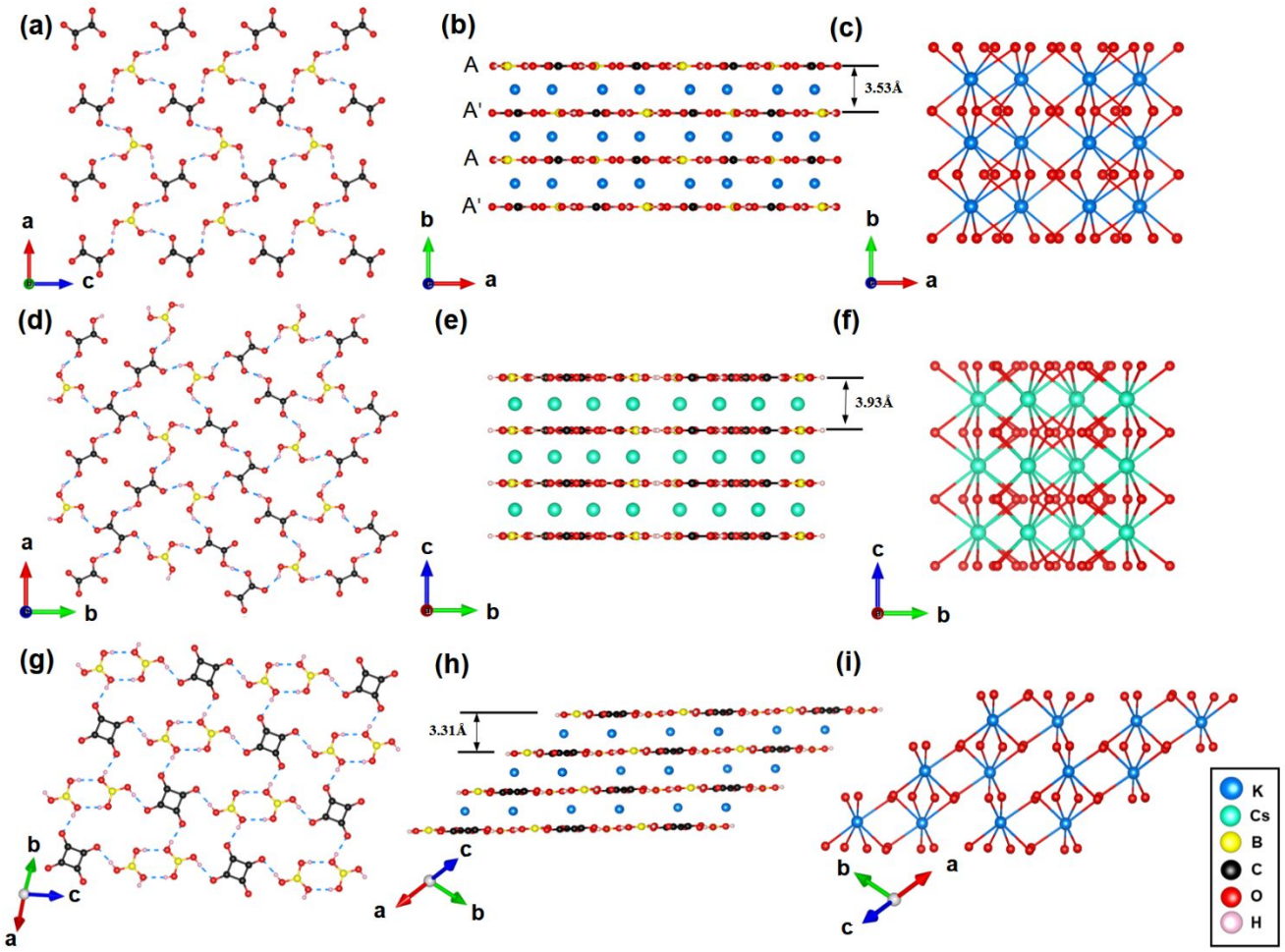

Figure 1. Ball and stick representation of the layer (a, d, g), the 3D frame (b, e, h) and the coordination environment of K^+/Cs^+ cations (c, f, i) for Ⅰ, Ⅱ and Ⅲ, respectively.

Ⅰ crystallizes in the centrosymmetric space group *Pnma* (No. 62) of the orthorhombic system. The structure is shown in Figures 1a–1c. As shown in Figure 1a, the planar $[B(OH)_3]$ and $[C_2O_4]^{2-}$ units are connected via O–H···O hydrogen bonds, forming a layer spreading in the ac-plane (labeled as Layer A). Layer A' is obtained by rotating A layer 180 ° about b-axis. Then Layers A and A' alternate along the b-axis to form the stacking mode of "AA'AA'…" (Figure 1b). Each K atom is coordinated with eight O atoms and is distributed in the interlayers (Figure 1c).

Ⅱ crystallizes in the centrosymmetric space group *Pbam* (No. 55) of the orthorhombic system. The structure is shown in Figures 1d–1f. As shown in Figure 1d, the layer consists of $[B(OH)_3]$, $[C_2O_4]^{2-}$ and $[HC_2O_4]^-$ connected by O – H ···O hydrogen bonds. Then the layers stack along the c-axis (Figure 1e). Figure 1f shows each Cs atom is coordinated with ten O atoms and is distributed in interlayers. Owing to larger atomic radius of Cs^+ cations compared with K^+ cations, Ⅱ exhibits a larger interlayer distance than Ⅰ (3.53 Å for Ⅰ, 3.93 Å for Ⅱ).

Ⅲ crystallizes in the centrosymmetric space group $P\bar{1}$ (No. 2) of the triclinic system. The structure is shown in Figures 1g–1i. As shown in Figures 1g and 1h, The planar $[B(OH)_3]$ and $[C_4O_4]^{2-}$ units are connected via O–H···O hydrogen bonds, forming a planar layer, and the layers stack in a certain direction with a slight translation across the face, resulting in non-perfect alignment. Each K atom is coordinated with seven O atoms and is distributed in the interlayers (Figure 1i).

It can be seen clearly from the above description, the anion units of the three compounds all exhibit layered structures. The introduction of $[B(OH)_3]$ restricts the arrangement of the surrounding C–O units to a planar layer. In order to determine

the impact of $[B(OH)_3]$ on arrangement, we compared the structure of **Ⅰ** and the oxalate without $[B(OH)_3]$, $K_2C_2O_4$.[15] For $K_2C_2O_4$ and **Ⅰ**, their $[C_2O_4]^{2-}$ units all exhibit pseudo-layered structures, and the angle between neighboring C–C bonds in the same layer is 79.69 and 50.57 °, respectively (Figure S4). Namely, the introduction of $[B(OH)_3]$ makes the orientation of C–C bonds more consistent and optimizes the arrangement of the $[C_2O_4]^{2-}$ units, which is favorable for generating a large optical anisotropy. Similar conditions can be found in structural comparison of KHC_2O_4[16] and $KHC_2O_4{\cdot}B(OH)_3$.[17] From KHC_2O_4 to $KHC_2O_4{\cdot}B(OH)_3$, the angle between neighboring C–C bonds decreases from 70.26 to 4.7 °. Owing to the directional interaction of hydrogen bonds, it can be concluded that, the assembly of $[B(OH)_3]$ and C–O units not only favors the formation of laminated structures, but also regulates the orientation of C–C bonds.

The crystals of **Ⅰ**, **Ⅱ** and **Ⅲ** were successfully synthesized by solvent evaporation methods (see the Supporting Information for experimental details). The sample purities were confirmed by the powder X-ray diffraction measurement (Figure S1). The results of the thermogravimetric (TG) and differential scanning calorimetry (DSC) of **Ⅰ**, **Ⅱ** and **Ⅲ** are shown in Figure S3. The endothermic peaks are at 192, 180 and 184 °C, respectively and their total weight loss rates are about 11.43, 7.80 and 16.56 %, respectively. The total weight loss rates can be attributed to the removal of 1.5, 4 and 1.5 water molecules from $[HC_2O_4]^-$ and $[B(OH)_3]$, respectively.

The IR spectra of three compounds are shown in Figure S2. The attribution of absorption peaks can be explained according to the reported compounds.[12,14,18–20] The strong absorption peaks appearing at 3674/2980/2906 cm^{-1} for **Ⅰ** and 3743/3029 cm^{-1} for **Ⅱ** can be attributed to the asymmetric stretching of the OH^- units. Bands arising from the characteristic C=O bonds are observed at 1863/1599 for **Ⅰ** and 1780/1739/1604 cm^{-1} for **Ⅱ**, respectively. Peaks observed at 1434/1402/1308/1239/1067/966 for **Ⅰ** and 1406/1312/1237/1072/927 cm^{-1} for **Ⅱ** are caused by the stretching vibrations of the C–O bonds. The absorption peaks appeared at 3745/3172/2925 cm^{-1} in **Ⅲ** can be attributed to the asymmetric stretching the OH^- units. The stretching vibrations of C=O bonds can be observed at 1741 cm^{-1}. The stretching C–O bonds can be observed at 1500/1432/1248/1179/1081 cm^{-1}. The absorption centered at 1500 cm^{-1} is produced by the overlap of C–O and C–C bond stretching vibrations in $C_4O_4^{2-}$. Bands from 900 to 500 cm^{-1} can not be easily distinguished because of the deformation vibration of $[C_2O_4]^{2-}$/$[HC_2O_4]^-$ /$[C_4O_4]^{2-}$ and the bending vibrations of the $[BO_3]$ group overlap.[13,14]

The transmittance spectra of **Ⅰ** and **Ⅲ** were measured based on the millimeter-sized crystals (Figures 2a and 2c). It demonstrates that the UV cutoff edge of **Ⅰ** and **Ⅲ** is 283 and 320 nm, respectively. The UV-vis-NIR diffuse reflectance spectrum of **Ⅱ** is shown in Figure 2b. Reflectance data are converted to absorbance (K/S) with the Kubelka-Munk function and the experimental band gap can be determined from the Tauc plot to be 4.17 eV.[21] It indicates that three compounds hold potential as short-wavelength optical materials.

To elucidate the relationship between microscopic structure and properties, the electronic structure calculations using GGA functionals were performed. As shown in Figure S5, **Ⅰ**, **Ⅱ** and **Ⅲ** exhibit band gaps of 3.47, 3.19 and 3.21 eV, respectively, which are underestimated compared with the experimental values because of a discontinuity in the exchange correlation energy functional.[22] The birefringence of **Ⅰ**, **Ⅱ** and **Ⅲ** was calculated to be 0.226, 0.167 and 0.346@1064 nm, respectively (Figures 2d–2f). Among the reported borates assembled with C–O units, $KHC_2O_4{\cdot}B(OH)_3$ (0.164@1064 nm),[17] $Rb_3(COOH)_3(H_3BO_3)_2$ (0.09@1064 nm),[14] and $Cs_3(COOH)_3(H_3BO_3)_2$ (0.10@1064 nm),[14] **Ⅰ**, **Ⅱ** and **Ⅲ** exhibit a rather large birefringence. Among three compounds, **Ⅲ** exhibits the largest value of birefringence. The largest orbital contributions in the top region of the valence band and bottom of the conduction band in these three compounds are mainly dominated by *p* orbitals of C and O atoms (Figures S5d–S5i). As is widely known, the optical properties of the compound mainly originate from the electronic transition between states around the Fermi level, so we primarily analyzed the region of valence band top and conduction band bottom. It can be concluded that the band gaps of three compound are mainly determined by C–O units and the birefringence mainly attributed to C–O units with large polarization anisotropy and their consistent alignment.

In conclusion, by assembling π-conjugated $[B(OH)_3]$ and C–O groups, $[C_2O_4]^{2-}$, $[HC_2O_4]^-$ and $[C_4O_4]^{2-}$, three new compounds, $K_2C_2O_4{\cdot}B(OH)_3$, $Cs_4(HC_2O_4)_2(C_2O_4){\cdot}[B(OH)_3]_2$ and $K(C_4O_4)_{0.5}{\cdot}B(OH)_3$ were synthesized. The introduction of $[B(OH)_3]$

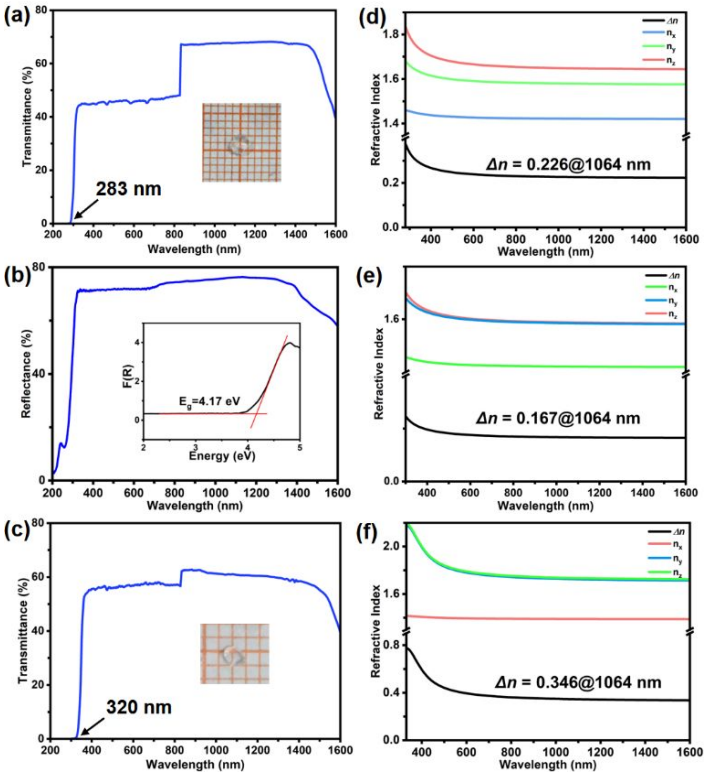

Figure 2. The transmittance spectra, the UV-vis-NIR diffuse reflectance (a, b, c), and the refractive indexes for Ⅰ, Ⅱ and Ⅲ, respectively (d, e, f).

extends the parallel layers of π-conjugated C–O groups and optimizes the arrangement of C–O groups due to the directional interaction of hydrogen bonds. The parallel arrangement of $[B(OH)_3]$ groups and C–O groups is conducive to superposition of the microscopic anisotropic polarizability, resulting in the large birefringence for these compounds. It is expected that structural optimization via combining $[B(OH)_3]$ with different π-conjugated C–O units can be adopted as a strategy to design UV birefringent material.

This work was supported by the National Key Research Project (2022YFE0134500), the CAS Youth Interdisciplinary Team (JCTD-2022-19), the National Natural Science Foundation of China (22335007, 22361132544), the Tianshan Innovation Team (2022TSYCTD0005), the Xinjiang Major Science and Technology Project (2021A01001), and the US National Science Foundation (DMR-1904701).

Data availability

The data supporting this article have been included as part of ESI.†.

Conflicts of interest

There are no conflicts to declare.

Notes and references

1 (a) K. M. Ok, Acc. Chem. Res., 2016, 49, 2774–2785;(b) Z. G. Xia, K. R. Poeppelmeier, *Acc. Chem. Res.*, 2017, **50**, 1222−1230;(c) M. Mutailipu, K. R. Poeppelmeier and S. L. Pan, *Chem. Rev.*, 2021, **121**, 1130−1202;(d) B. L. Cheng, Z. J. Li, Yu Chu, A. Tudi, M. Mutailipu, F. F. Zhang, Z. H. Yang, S. K. Pan, *Natl. Sci. Rev.*, 2022, **9**, nwac110;(e) P. S. Halasyamani and J. M. Rondinelli, *Nat. Commun.*, 2018, **9**, 2972;(f) F. Liang, L. Kang, Z. S. Lin and Y. C. Wu, *Cryst. Growth Des.*, 2017, **17**, 2254–2289;(g) A. Tudi, Z. J. Li, C. W. Xie, T. Baiheti, E. Tikhonov, F. F. Zhang, S. L. Pan, Z. H. Yang, *Adv. Funct. Mater.*, 2024, **34**, 2409716.

2 (a) G. H. Zou and K. M. Ok, *Chem. Sci.*, 2020, **11**, 5404−5409;(b) H. Zhou, M. Cheng, D. D. Chu, X. Liu, R. An, S. L. Pan, Z. H. Yang, *Angew. Chem. Int. Ed*., 2024, **63**, e202413680;(c) M. Zhang, D. H. An, C. Hu, X. L. Chen, Z. H. Yang and S. L. Pan, *J. Am. Chem. Soc*. 2019, **141**, 3258–3264; (d) F. F. Zhang, X. L. Chen, M, Zhang, W. Q. Jin, S. J. Han, Z. H. Yang and S. L. Pan, *Light Sci Appl.*, 2022, **11**, 252; (e) Y. Wang, B. B. Zhang, Z. H. Yang and S. L. Pan, *Angew. Chem. Int. Ed.*, 2018, **57**, 2150–2154.

3 (a) F. Sedlmeir, R. Zeltner, G. Leuchs and H. G. L. Schwefel, *Opt. Express.*, 2014, **22**, 30934–30942;(b) H. T. Luo, T. Tkaczyk, E. L. Dereniak, K. Oka and R. Sampson, *Opt. Lett.*, 2006, **31**, 616–618;(c) J. R. Devore, *J. Opt. Soc. Am.*, 1951, **41**, 416–419;(d) B. B. Zhang, G. Q. Shi, Z. H. Yang, F. F. Zhang, S. L. Pan, *Angew. Chem. Int. Ed*., 2017, **56**, 3916 – 3919;(e) Z. Z. Zhang, Y. Wang, B. B. Zhang, Z. H. Yang and S. L. Pan, *Angew., Chem. Int. Ed.*, 2018, **57**, 6577–6581;(f) B. H. Lei, S. L. Pan, Z. H. Yang, C. Cao and D. J. Singh, *Phys. Rev. Lett.*, 2020, **125**, 187402.

4 (a) C. H. Hu, J. J. Liu, J. L. Chu, J H. Hu and X. Z. Jiang, *J. Saudi Chem. Soc.*, 2024, **28**, 101789;(b) M. Mutailipu, M. Zhang, B. B. Zhang, L. Y. Wang, Z. H. Yang, X. Zhou, S. L. Pan, *Angew. Chem. Int. Ed*., 2018, **57**, 6095–6099;(c) M. Cheng, W. Q. Jin, Z. H. Yang and S. L. Pan, *Chem. Sci.*, 2022,**13**, 13482–13488; (d) A. Tudi, S. J. Han, Z. H. Yang and S. L. Pan, *Coordin. Chem. Rev*., 2022, **459**, 214380.

5 (a) W. B. Zhang, X. P. Shi, R. An, A. Tudi, Z. H. Yang, S. J. Han and S. L. Pan, *Mater. Today Chem.*, 2024, **37**, 102005;(b) H. W. Jia, D. Xu, Z. J. Li, M. Arif, Y. S. Jiang and X. L. Hou, *Inorg. Chem. Front*., 2024, DOI: 10.1039/d4qi01061b;(c) L. Y. Zhang, S. B. Wang, F. F. Zhang, Z. H. Yang and X. L. Hou, *Dalton Trans.*, 2023, **52**, 13492–13496;(d) Y. Q. Li, X. Zhang, J. Y. Zheng, Y. Zhou, W. Q. Huang, Y. P. Song, H. Wang, X. Y. Song, J. H. Luo and S. G. Zhao, *Angew. Chem. Int. Ed.*, 2023, **62**, e202304498.

6 (a) W. B. Zhang, X. L. Hou, S. J. Han, S. L. Pan, *Coordin. Chem. Rev.*, 2024, **505**, 215664;(b) Y. C. Liu, Y. G. Shen, S. G. Zhao and J. H. Luo, *Coordin Chem Rev.* 2020, **407**, 213152;(c) G. Q. Shi, Y. Wang, F. F. Zhang, B. B. Zhang, Z. H. Yang, X. L. Hou, S. L. Pan and K. R. Poeppelmeier, *J. Am. Chem. Soc.*, 2017, **139**, 10645–10648;(d) H. T. Qiu, F. M. Li, Z. Li, Z. H. Yang and S. L. Pan, M. Mutailipu, *J. Am. Chem. Soc.*, 2023, **145**, 24401–24407;(e) R. K. Li, Y. Y. Ma, *CrystEngComm*, 2012, **14**, 5421.

7 (a) X. F. Wang, Y. Wang, B. B. Zhang, F. F. Zhang, Z. H. Yang and S. L. Pan, *Angew. Chem. Int. Ed.*, 2017, **56**, 14119–14123; (b) X. F. Wang, Y. Li, Z. L. Chen, J. Y. Li, F. F. Zhang, K. R. Poeppelmeier, S. L. Pan and K. M. Ok, *Small Struct.*, 2023, **4**, 2300274; (c) W. C. Li, J. B. Wang, L. L. Liu, C. M. Huang, Y. Y. Ding, M. M. Zhu, J. D. Tian, H. X. Qi, Y. Q. Chu and J. Y. Xu, *Inorg. Chem.*, 2024, **63**, 8408–8417; (d) M. Cheng, W. Q. Jin, Z. H. Yang and S. L. Pan, *Chem. Sci.*, 2022, **13**, 13482–13488; (e) A. Tudi, S. J. Han, Z. H. Yang, S. L. Pan, *Coord. Chem. Rev*., 2022, **459**, 214380;(f) J. Chen, M. B. Xu, H. Y. Wu, J. Y. Wu and K. Z. Du, *Angew. Chem. Int. Ed.*, 2024, DOI: 10.1002/anie.202411503;(g) M. B. Xu, J. Chen, H. Y. Wu, J. J. Li, N. Yu, M. F. Zhuo, F. F. Mao and K. Z. Du, *Inorg. Chem. Front.*, 2024, **11**, 4307–4317;(h) M. B. Xu, Q. Q. Chen, B. X. Li, K. Z. Du and J. Chen, *Chin. Chem. Lett.*, 2024, DOI: 10.1016/j.cclet.2024.110513.

8 T. H. Tong, W. Y. Zhang, Z. H. Yang and S. L. Pan, *Angew Chem., Int Ed.*, 2021, **60**, 1332–1338.

9 H. M. Wang, Q. Wang, Q. Wang, L. L. Cao, L. Huang, D. J. Gao, J. Bi and G. H. Zou, *Cryst. Growth Des*., 2022, **22**, 4236–4242.

10 L. N. Kholodkovskaya, V. K. Trunov and N. B. Tskhelashvili, *J. Struct. Chem.*, 1990, **31**, 509–511.

11 W. Clegg, *Z. Kristallogr.*, 1984, **169**, 211–217.

12 D. Yan, Y. Ma, H. H. Huang, B. B. Zhang, R.-L. Tang, L. Hu, F.-F. Mao, J. Zheng, X.-D. Zhang and S.-F. Li, *Chem. Commun.*, 2023, **59**, 219–222.

13 Y. L. Deng, L. Wang, Y. W. Ge, L. Huang, D. J. Gao, J. Bi and G. H. Zou, *Chem. Commun.*, 2020, **56**, 9982–9985.

14 Y. Q. Guo, D. Zhang, T. Zheng, L. Huang, D. J. Gao, J. Bi and G. H. Zou, *Cryst. Growth Des.*, 2021, **21**, 5976–5982.

15 R. E. Dinnebier, S. Vensky, M. Jansen and J. C. Hanson, *Chem. Eur. J.*, 2005, **11**, 1119–1129.

16 H. Einspahr, R. E. Marsh and J. Donohue, *Acta Crystallogr.*, 1972, **B28**, 2194–2198.

17 Y. Li, J. Lee and K. M. Ok, *Bull Korean Chem Soc.*, 2023, **44**, 788–793.

18 H. M. Wang, Q. Wang, Q. Wang, L. L. Cao, L. Huang, D. J. Gao, J. Bi and G. H. Zou, *Cryst. Growth Des.*, 2022, **22**, 4236–4242.

19 C. C. Jin, F. M. Li, X. Q. Li, J. J. Lu, Z. H. Yang and S. L. Pan, M. Mutailipu, *Chem. Mater.*, 2022, **34**, 7516–7525.

20 L. Y. Ren, L. H. Cheng, X. Y. Zhou, J. X. Ren, L. L. Cao, L. Huang, X. H. Dong, Y. Q. Zhou, D. J. Gao and G. H. Zou, *Inorg. Chem. Front.*, 2023, **10**, 5602–5610.

21 J. Tauc, *Mater. Res. Bull.*, 1970, **5**, 721–729.

22 R. W. Godby, M. Schlüter and L. J. Sham, *Phys. Rev. B*, 1987, **36**, 6497–6500.

The data supporting this article have been included as part of ESI.†.